DOI: https://doi.org/10.3126/jhm.v13i1.95552

Journal of Hydrology and Meteorology
Vol. 13, No. 1, December 2025

Assessment of Run-off-River Hydropower Potential in a Glacier-Fed Catchment Using a Glacio-Hydrological Degree-day Model: A Case Study of Budhigandaki River Basin, Nepal

Sabina Twayana[1], Sagar Lamichhane[1*], Rijan Bhakta Kayastha[2], and Rakesh Kayastha[2]
[1]Department of Environmental Science and Engineering, School of Science, Kathmandu University
[2]Department of Environmental Science and Engineering, Himalayan Cryosphere, Climate and Disaster Research Center (HiCCDRC), School of Science, Kathmandu University

Corresponding author:* Sagar Lamichhane, sagarlamichhane74@gmail.com

ABSTRACT
Assessment of hydropower potential is crucial which enable associated stakeholders for financial investments in future production of electricity. Discharge estimation plays a key role in assessing hydropower potential. Glacio-hydrological Degree-day Model (GDM), which is widely acknowledged fully distributed model used to calculate discharge in glacierized river basins, including those with debris-covered glaciers, and is noted for its computational efficiency. This study aimed to assess run-off river hydropower potential using this model. The research was conducted in three stages, literature review and data preparation in the first phase, model calibration and validation in the second phase and identifying possible hydropower sites, assessing their potential, and forecasting future discharge under the SSP2-4.5 and SSP5-8.5 scenarios in the third phases. The Budhigandaki River basin (BGRb) was chosen as a case study region in order to achieve the study's goal. The modeling period's NSE and VD values were 0.84 and -9.35 %, respectively; the validation period's NSE and VD values were 0.86 and -8.62 %. This suggests that the model is performing satisfactorily. From 2000 to 2015, this analysis found 35 possible locations with a combined capacity of 6,308 MW at a 40 % flow exceedance. Additionally, the average increase in simulated discharge is 8.88 % and 42.6 %, respectively, according on the results of the future prediction of discharge and contribution of various components using two climatic scenarios, SSP2-4.5 and SSP5-8.5, for the period of 2020–2100. In the context of changing climatic condition, this study helps to fulfill the increasing demand for renewable energy and efficiently manage water resources.

Keywords: Glacio-hydrological modeling, renewable energy, flow projection, climate scenarios, water resource management

1. Introduction

With the increasing global need for clean and sustainable energy, researchers are driving towards renewable sources of energy that encompasses hydropower, wind, solar, bioenergy, tidal. Among these, hydropower emerges as a dependable and established option means to mitigate climate change in diminishing reliance on fossil fuels (Calheiros et al., 2024). However, fossils fuels are still significantly used across the world to address current energy demands (Halkos & Gkampoura, 2023). To fully utilize the hydropower resources, it required detailed assessment from technical, economic, social, and environmental aspects (Zhang et al., 2021). According to the study carried out by Spanoudaki et al., (2022), assessing the hydropower potential is an instrumental that enables various associated stakeholders to acquire financial investments for future electricity production. In the last 20 years, research activities on assessment of hydropower potential have been significantly increasing across every engineering domain that entails environmental, civil, mechanical, and electrical. However, there are still numerous challenges in accurate estimation of hydropower production potential because it is driven by complex factors that includes climate change, population, socio-economic development, technological development, rules and regulations of state (Calheiros et al., 2024).

To assess hydropower potential there are various types of models/approaches. For instance, Pandey et al., (2015) and Pokharel et al., (2020) has integrated spatial technology and Soil and Water Assessment Tool (SWAT) model for assessing hydropower potential. Similarly, Kouadio et al., (2022) has coupled SWAT and Quantum Geographic Information System (QGIS) known as QSWAT to determine the potential of hydropower sites for future hydropower development in watershed regions. Furthermore, Spanoudaki et al., (2022) has leverage Bayesian and Stochastic approaches for streamflow simulation. Similarly, a widely acknowledged model, Hydropower Potential Assessment Tool (HPAT) has been adapted by Mosier et al., (2016) to evaluate the run-of-river resource potential for hydropower generation. Furthermore, there is also a model called as Glacio-hydrological Degree-day Model (GDM) that also stimulate and predict the daily discharge of the glaciated mountain basin (Kayastha et al., 2019). This model is based on the faster and efficient discharge calculation principle whereas other models such as SWAT, QSWAT, HAST rely on time consuming computational methods (Kayastha & Kayastha, 2020). This model streamlines the assessment process and provides valuable insights into the dynamics of river systems, particularly in regions like the Himalayas where understanding the impacts of climate change on hydrological systems is of paramount importance (Kayastha & Kayastha, 2019).

According to Shrestha (1966), Nepal has 83,500 MW of hydropower potential overall, with 114 site

having a economical feasibility of 45,610 MW capacity. In addition, a recent research showed that Nepal has a 53,836 MW of run-of-river (ROR) hydropower potential with a 40 % dependable flow (Jha, 2010; Shrestha 1996; Pradhan, 2009; WECS, 2011). Jha, (2010) calculated the total theoretical ROR hydropower potential of Nepal as 53,836 MW at a flow of 40% Probability of Exceedance (PoE) and 80% efficiency using the Shuttle Radar Topographic Mission (SRTM) Digital Elevation Model (DEM) resampled at 100 m resolution and the Catchment Area Ratio (CAR) method to estimate river discharge at ungauged locations. (Bajracharya, 2015) calculated Nepal's Gross Renewable Hydropower (GRHP) to be 103,341 MW at mean annual flow using the Soil Water Assessment Tool (SWAT) hydrological model and the Advanced Spaceborne Thermal Emission and Reflection Radiometer Global-DEM (ASTER G-DEM) with a resolution of 30 m.

The current study conducted by WECS in 2019 on Nepal's hydropower potential assessed the GRHP at 72,544 MW at a 40% PoE, utilising the Hydrologic Engineering Center-Hydrological Modelling System (HEC-HMS) model and ASTER G-DEM with a 30 m resolution. Prajapati, (2015) calculated the ROR hydropower potential of the Karnali River basin to be 14,150 MW at 40% PoE, 84% efficiency, and 10% seasonal outage and riparian release using HEC-HMS and a reclassified DEM with a resolution of 100 m. Aryal et al., (2018) estimated the overall power potential of the Bagmati River basin for flows of various PoE and identified possible sites using the SWAT model and SRTM DEM of 90 m resolution. Kayastha et al., (2024) identify a total of 116 and 83 suitable sites wih 4242 and 3823 MW power potential of BRb and MRb using Glacio hydrological Degree-Day Model at 40% dependable flow. Bhattarai et al., (2024) identify 36 sites across stream of order 3,4,5 yeilding a potential of 371.30 MW at a 40% PoE using integrated approach combining SWAT-based hydrological modeling within a GIS in Sunkoshi River Basin. Joshi & Mishra, (2024) used SWAT modeling and Arc GIS to estimate run of river hydropower potential in Marsyangdi River basin results 1569.89 MW and 2191.68 MW at 40 % and 30 % PoE.

Although GDM has been widely used for discharge simulation in glacier-fed basins, its integration into hydropower potential assessment remains largely unexplored in Nepal. This study bridges that gap by coupling GDM-derived discharge with standard hydropower estimation approaches. The glacio-hydrological model is used solely to simulate discharge, which serves as the fundamental input for hydropower estimation. Therefore, to address this existing research gap, the aim objective is to estimates the theoretical Run-off-River (RoR) hydropower potential of the Budhigandaki River Basin (BRB) using GDM. The theoretical hydropower potential refers to the total energy obtainable from available discharge and hydraulic head without considering economic, environmental, or technical constraints. Therefore, our current study is crucial for obtaining information of future hydrological conditions and the contribution of water balance components (rain, baseflow, snowmelt, and icemelt) to river discharge in all of the BGRB sub-basins under various SSPs climate scenarios for the basin.

2. Study area

BGRb is situated in western Nepal and serves as a significant tributary of the Gandaki River basin, with its source originating from the Himalayas in the northern region is shown in Figure 1. It lies between latitudes 27°50' and 28°00' N and longitudes 84°30' and 85°10' E. The total area of BGRB is 3881.16 square kilometers. About one-fourth of the basin area lies in the Tibetan Plateau of the People's Republic of China, and the remaining part lies in the Federal Democratic Republic of Nepal (Marahatta, 2022). Most of it lies in the Gorkha District of Nepal, with altitudes ranging from 479 meters above sea level at the Arughat hydrological station to 8,163 meters above sea level at the top of the basin, Mount Manaslu. There are three types of climatic zones found in the river basin, temperate climate with dry winter and warm summer (312m - 3500 m), polar tundra (3500m - 6500 m) and polar frost (6500m - 8147m) (Karki et al., 2020). Snow and glaciers make up 29% of BGRb, followed by forest (23%), barren (21%), shrub and grassland (18%), and farmland (8%). The smallest percentage (~1%) of the overall land is made up of residential built-up area and rivers.

The dominant soil types in the lower and middle valleys are sandy loam and silty loam, while the upper regions consist mainly of glacial till and coarse-textured morainic deposits. The major rivers of the Budhigandaki River are Syar, Tom (Dogar), and Ankhu Khola. The other tributaries of the Budhigandaki are Larke, Athahra Saya, Phurba Dhyapsa, Hinan, Gungan, Sanchu, Seran, Udilun, Sayale, Sanamchu, Chulung, Bhalu, Yaru, Pangair, Dowan, Namrung, Machi, Richet, Aarkhet, Kaste, and Jyadul Khola (Marahatta, 2022). The mean annual flow of the Budhigandaki River upstream of the Trishuli confluence is estimated as 240 m^3/s (Marahatta, et al., 2021).

3. Input Datasets

3.1 Meteorological and Hydrological data

Daily precipitation data of six stations (Jagat, Larke Sambo, Gorkha, Chhekampar, Gharedhunga, Arughat), minimum and maximum temperature data from two stations (Gorkha, Timure), and daily discharge data (Arughat) from one station for the period 2000-2015 were obtained from the Department of Hydrology and Meteorology (DHM). Although the Gorkha, Gharedhunga, and Timure stations are located outside the delineated catchment boundary, their data were incorporated into the GDM model due to the limited availability of spatially distributed climate records within the basin. These stations provided essential climatic inputs for improving the spatial representation

of meteorological conditions necessary for accurate hydrological modeling.

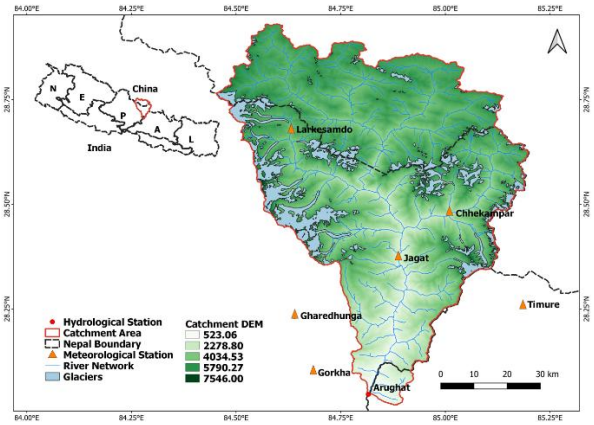

Figure. 1. Locations of the Budhigandaki River basin in Nepal (Nepal is in the inset).

3.2 Spatial data

Similarly, to create the DEM of the case study area, a publicly available 30m spatial resolution of the DEM (Shuttle Radar Topography Mission) was acquired through USGS. GDM-based land use and cover was used and categorized into eight categories, L1, L2, L3, L4, L5, L6, L7, L8. The indication of each category is L1; land covered by forest, L2; land covered by agriculture, L3; grassland, L4; bare land, L5; waterbodies, L6; built-up, L7; debris glacier, and L8; glacier.

3.3 Input Parameters, GDM Modeling and Evaluation

To successfully execute the GDM, parameters need to be adjusted properly. These includes start_date, end_date, start_timesteps, end_timesteps, lat_deg, delta_gwsh, delta_gwdp, alpha_gwsh, alpha_gwdp, beta_dp, Kx, Tc, and Kd. Initially, these parameters values were defined based on existing similar studies available through the journal papers and reports. Then after, using the inputs and defined parameters, GDM was executed for the year 2000-2007. Then after, the model's performance was assessed, and results were not satisfactory. Following this, parameters were adjusted and again the model was re-executed. This process was carried out iteratively until the model was able to perform well. After successfully obtaining desired model performance, adjusted parameters were determined. Using these adjusted parameters model was further validated for the year 2008-2015.

3.4 Future climate data

The collection of five GCMs (ECEARTH3, INM-CM-8, MPI-ESM1-2-HR, NORESMMM, INM-CM5-0) provides daily temperature and daily precipitation data for the future climatic scenarios used in this study. Two scenarios for climate projections (SSP2-4.5, SSP5-8.5) were chosen to replicate discharges in the future. These two scenarios were chosen primarily to describe the technological, socioeconomic, and demographic factors that underlie the anthropogenic greenhouse gas emissions that lead to climate change. Bias correction was used to apply GCM forecasts at the local scale once SSP2-4.5 and SSP5-8.5 were chosen. The bias on daily precipitation and temperature series data were corrected using the methods given by (Weiland et al., 2010). The future hydrological regime was estimated through model simulation using temperature and precipitation forecasts from the SSP2-4.5 and SSP5-8.5 climatic scenarios. Temperature lapse rate and precipitation gradient were used to distribute the daily time series temperature and precipitation data for two distinct scenarios to grids according to elevation at the reference station.

4. Methods

4.1 Glacio-hydrological Degree-day Model (GDM)

A distributed and gridded glacio-hydrological model that can simulate the contribution of hydrological components to river flow is the Glacio-hydrological Degree-day Model (GDM, Version 2). Glacier ice melt, snowmelt, rainfall, and baseflow are the four distinct run-off components that GDM simulates in total discharge at daily time steps. A melt module is based on degree-day approach, a simplification of complex process (Braithwaite & Olesen, 1989) to estimate the glacier ice and snow melts with minimal data requirements (Kayastha et al., 2006). The concept of two reservoir-based modelling approaches of Soil and Water Assessment Tool (SWAT) is adopted to simulate the hydrological response of baseflow and rainfall runoff contribution in river discharge (Luo et al., 2012). The model for the discharge simulation is forced by daily projected temperature and precipitation from the reference station to each grid. In each grid during the corresponding time step, the threshold temperature (TT) establishes whether the precipitation is rain or snow as follows: -

$$Precipitation = \begin{cases} rain, if\ T \geq T_T \\ snow, if\ T \leq T_T \end{cases}$$

where TT is the threshold temperature and T is the estimated daily air temperature for grids, both expressed in °C. Daily snowmelt from glacierized and glacier-free regions, as well as ice melt from debris-free and debris-covered ice, are computed in each grid as follows:

$$M = \begin{cases} K_d\ or\ K_{s\ or}\ K_b \times T & if, T > 0 \\ 0 & if, T \leq 0 \end{cases}$$

where T is the daily air temperature in °C, M is the ice or snow melt in mm day^{-1} in each grid, and K_d, K_s, and K_b are the degree-day factors for clean glacier ice, debris-covered ice, and snow in mm °C^{-1} day^{-1}. The multilayer melting of snow over both clean and debris-covered ice is taken into consideration by the model.

Baseflow is calculated using a baseflow simulation approach as in SWAT. Two aquifer system shallow and deep aquifer system concept is applied to simulate the baseflow in glacier and snow melt dominated basin (Luo et al., 2012; Zhang et al., 2015). The advantage of

two reservoir systems over single reservoir system is that it releases the discharge in recession period and assures the level of discharge much more similar to observed discharge during the recession period.

Hence, Luo et al., (2012) baseflow method is used in this study's baseflow simulation. The amount of surface water percolation, W_{seep}; the delay time for the overlying geological formation for shallow aquifer percolation, $\delta_{gw,\ sh}$; the recession constant for shallow aquifer, $\alpha_{gw,\ sh}$; the seepage constant for deep water percolation, β_{dp}; the delay time for deep aquifer percolation, $\delta_{gw,\ dp}$; and the recession constant for deep aquifer, $\alpha_{gw,\ dp}$, are the main factors taken into account in baseflow simulation. Neitsch et al. (2011) and Luo et al. (2012) provide specifics about the baseflow technique and parameter settings.

Each grid's runoff from rainfall, snowmelt, and icemelt contributes to the surface runoff, or Q_G. Grid-wise calculations of the surface runoff component are made using the following formula.

$$Q_G = Q_r * C_r + Q_s * C_s + Q_i$$

where Q_G is the surface runoff component from each grid in $m^3\ s^{-1}$, Q_r is the discharge from rain, Q_s is the discharge from snowmelt, and Q_i is the discharge from clean and debris-covered ice melt in $m^3\ s^{-1}$. C_r and C_s are the rain and snow coefficients. Next, the total baseflow contributions, Q_B from all grids, and the total surface runoff contribution, Q_R from all grids, are represented as follows:

$$Q_R = \sum_{G=1}^{n} Q_G$$

$$Q_B = \sum_{b=1}^{n} Q_b$$

where n is the number of grids and Q_b is the baseflow contribution from each grid. The baseflow contribution, Q_B, and the total surface discharge, Q_R, are then directed towards the outlet using the following formula

$$Q = Q_R * (1 - k) + Q_{R(d-1)} * k + Q_B$$

where d is the d^{th} day, Q is the total discharge in $m^3\ s^{-1}$, and k is the recession coefficient.

4.2 Model Performance Indices

The daily time series of observed and simulated discharges were compared in order to evaluate the model's performance efficiency. The Nash-Sutcliffe Efficiency (NSE) index is used to assess the model result between the simulated and observed discharge (Nash & Sutcliffe, 1970). Mathematically, it is represented as,

$$NSE = 1 - \frac{\sum_{i=1}^{d}(Q_{Obs} - Q_{sim})^2}{\sum_{i=1}^{d}(Q_{Obs} - Q_{avg})^2}$$

where Qavg is the average observed discharge, Qsim is the daily simulated discharge, and Qobs is the daily observed discharge.

Similarly, volume difference was also used to determine the model accuracy and was calculated by using the below equation ((Nash & Sutcliffe, 1970 ; (Kayastha & Kayastha, 2019).

$$VD = \frac{V_R - V'_R}{V_R} * 100$$

where, V'_R and V_R is the simulated and measured discharge respectively.

4.3 Assessment of Hydropower Potential

The Potential sites for hydropower projects were found using QGIS's geospatial tools. The stream networks and watersheds performed the pre-processing procedures for the hydrological study, including filling voids, flow directions, and accumulation. In order to determine a possible site for hydropower development and guarantee a steady water flow, the third order of stream was assessed using the Strahler method. A minimum distance of 7 km between the two consecutive hydropower plants was considered to provide adequate space for civil works and environmental considerations, such as reservoirs, powerhouses, and environmental flows (Kayastha et al., 2024). An elevation below 4,000 meters is considered to be feasible for hydropower project development because of its steepness, high gradient, and altitude. Using the DEM at the initial and terminating spots, the gross head of the stream segments was derived. The net or effective head, which was utilized for potential estimation in this study, was defined as 70% of the gross head. In this study, only heads larger than 20 meters were taken into account. FDC was used to estimate design flow (Q40) values of all the discharge of identified potential sites. Finally, hydropower potential of each identified sites was calculated using the mathematical relation, $P\ (Megawatt) = \rho.\ g.\ Q.\ h\ /\ 10^6$, where ρ is the density of water ($1000\ kg\ m^{-3}$), g is the gravitational acceleration ($9.81\ m\ s^{-2}$), Q is the discharge ($m^3\ s^{-1}$), and h is the net or effective head (m).

5. Results and Discussion

5.1 Calibration and Validation

The model was calibrated for the years of 2000-2008 while the validation years is 2009-2015. Table 1 illustrates the statistical assessment, which was shown through mean, standard deviation, NSE and VD of observed and simulated flows over the study periods.

Figures 2 and 3 represents the simulated and observed discharge during the 2000-2015 at Arughat station. These figures show that the model slightly overestimated during the low flow or pre-monsoon periods. This might be due to the varying distribution of precipitation.

Table 1. Statistical indexes, NSE, and VD of the observed and simulated series for model calibration and validation.

S.N.	Statistic (Years)	Mean Flow(m^3/s)		Standard Deviation(m^3/s)		Performance Indicators	
		Observed	Simulated	Observed	Simulated	NSE	VD
1.	Calibration (2000-2008)	146.46	127.41	156.97	136.27	0.84	-9.35
2.	Validation (2009-2015)	157.38	147.47	169.59	139.83	0.86	-8.62

It is possible that the model underestimated the amount of precipitation at high elevations since it was unable to identify a few peaks in the graph. According to Immerzeel et al., (2015) and Bocchiola et al., (2011) precipitation at glacier altitude maybe two to ten times higher than that of the valley bottoms, and the distribution of precipitation from the reference station at lower elevations to higher altitudes may not be properly representative. Additionally, according to Barry, (2012), the precipitation gradient in a mountainous environment appears to be changed both vertically and horizontally. Despite these limitations, the model was still able to replicate the daily discharge with excellent NSE values and within 20 % of the real volume despite the limited input datasets.

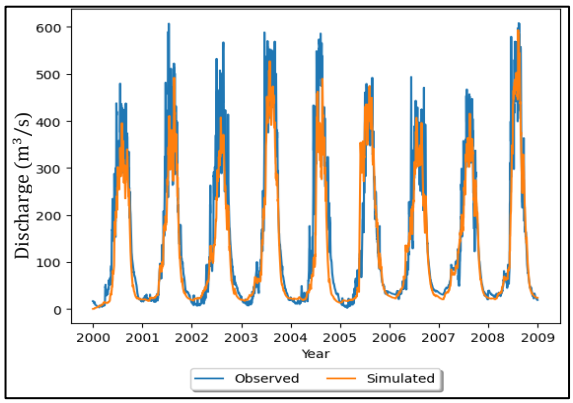

Figure. 2. The comparison of observed and simulated discharge hydrographs during calibration period.

5.2 Contributions of Ice Melt, Snow Melt, Baseflow and Rainfall to total Discharge

Figure 4 represents the mean monthly contribution of ice, snow melts (debris and clean), base flow and raiin during the calibration and validation periods. It shows during the peak season (June-September), all four contributors significantly enhance the discharge rate. For instance, in August, the discharge value reached the maximum, i.e. approximately 375 m^3/s.

Similarly, in July the discharge rate value was slightly lower than in August, i.e. approximately 360 m^3/s. Furthermore, in September, the discharge value was almost lower by a quarter than in August which is approximately equivalent to 275 m^3/s. Meanwhile, during pre-monsoon (April-May) the contributions of snow, ice melts (debris and clean), rain, and baseflow drastically decreased compared to the peak season where discharge rate are within 100 m^3/s.

Similarly, during post-monsoon (October and November) discharge rates are approximately 110 m^3/s and 45 m^3/s, respectively. It can certainly be noticed that perception significantly plays a pivotal role in affecting the discharge rate.

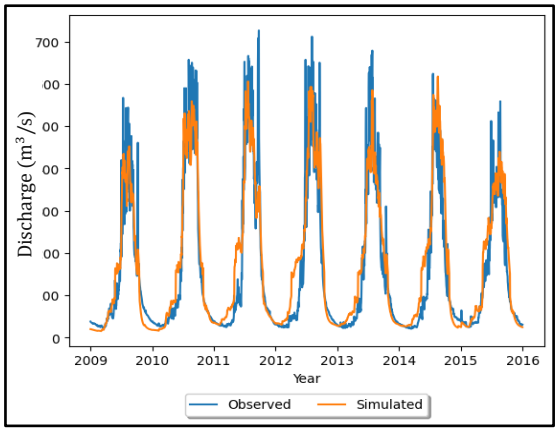

Figure. 3. The comparison of observed and simulated discharge hydrographs during validation period.

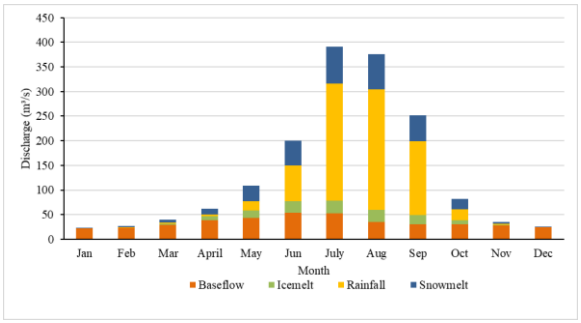

Figure. 4. Monthly contribution of Baseflow, Ice Melt, Rainfall, and Snow Melt to total river discharge in BGRB.

Figure5 illustrates the percentage of the contribution of discharge by the four contributors through a pie chart. It indicates 17.46 % of discharge was from snowmelt, whereas 6.7 % was from ice melt. (Sharma et al., 2020) calculated an average more than 60 % of total annual discharge is contributed by snowmelt during the peak months of May and June. Similarly, (Marahatta, et al., 2021) study results shows about 20 % of total flow is at the basin outlet is contributed by snowmelt during the pre-monsoon period and 8 % in the post monsoon period. Similarly, 22.30 % of the discharge was contributed through baseflow while 40.57 % was directly from rain being

the highest contributor. Rainfall contributes most to discharge in both basins during the season of monsoon (June- September), whereas baseflow contributes all year long, reaching its peak in the latter part of the monsoon. Similarly, ice melt's contribution to discharge is initiated during the pre-monsoon season, which is certainly due to temperature and precipitation.

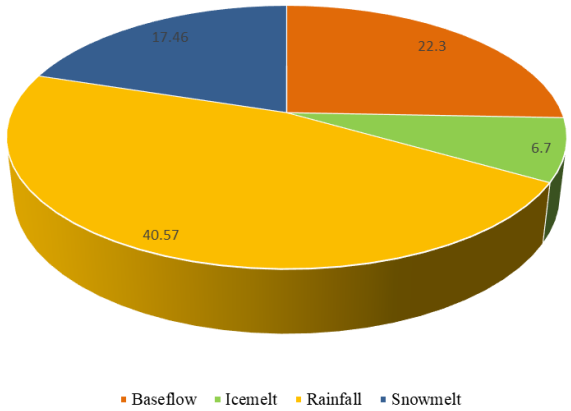

Figure 5. Percentage of contributors on total river discharge in BGRB.

5.3 Future Hydrological Regimes Under Different Climate Scenarios

The average yearly simulated flow at the outlet of BGRB for the baseline period (2000-2015) is 136 m^3/s. From 2020 to 2100, under SSP2-4.5, the flow increases to 148 m^3/s, reflecting an 8.8 % change from the baseline flow. This modest increase could be attributed to moderate changes in climate conditions and human activities as projected under SSP2-4.5. Conversely, under SSP5-8.5, the flow significantly rises to 194 m^3/s, representing a substantial 42.6 % change from the baseline flow. The SSP5-8.5 scenario, associated with higher emissions and more severe climate change impacts, projects a substantially greater percentage increase in water flow compared to SSP2-4.5. This suggests that the SSP5-8.5 scenario anticipates more pronounced alterations in hydrological regimes, potentially leading to heightened risks of flooding, changes in water availability, and impacts on ecosystems and human populations reliant on water resources. Conversely, while SSP2-4.5 also anticipates changes in water flow, they are comparatively less extreme, indicating a milder trajectory of environmental change. This significant increase indicates more drastic changes in climate conditions and socioeconomic factors as projected under SSP5-8.5, likely leading to greater water availability or changes in hydrological processes.

The observed trends in simulated discharge and its components shown in Figure 6 provide valuable insights into future hydrological dynamics in the BGRB. The increasing trend in discharge from approximately 2026 to 2035, followed by a decrease from around 2050 to 2060, likely reflects the complex interplay of climatic factors and hydrological processes. This fluctuation could be attributed to variations in precipitation patterns, temperature, and land use changes, affecting water availability and flow dynamics.

The alignment of rainfall data with discharge data suggests a direct relationship between precipitation and streamflow, highlighting the significant influence of rainfall on basin hydrology. This correlation underscores the importance of accurately modelling precipitation patterns for reliable hydrological projections and water resource management strategies. Furthermore, the constant trend line of snow melt throughout the year indicates a consistent contribution of snow melt to total discharge. This stability may result from consistent snow accumulation and melting patterns, regulated by factors such as altitude, temperature, and seasonal variability in snowpack dynamics. The persistence of snow melt underscores its role as a crucial water source, particularly in regions dependent on snow-fed rivers for freshwater supply and ecosystem sustainability.

Figure 7 shows in SSP2-4.5, baseflow accounts for the highest percentage contribution at 23.3 %, indicating that a significant portion of the water flow comes from groundwater discharge and other continuous sources. Rainfall follows closely behind at 61.8 %, suggesting that precipitation is the primary driver of water flow in this scenario, which is typical for regions with abundant rainfall. Snowmelt contributes 13.081 %, indicating that snow accumulation and subsequent melting also play a notable role, especially in regions with seasonal snow cover.

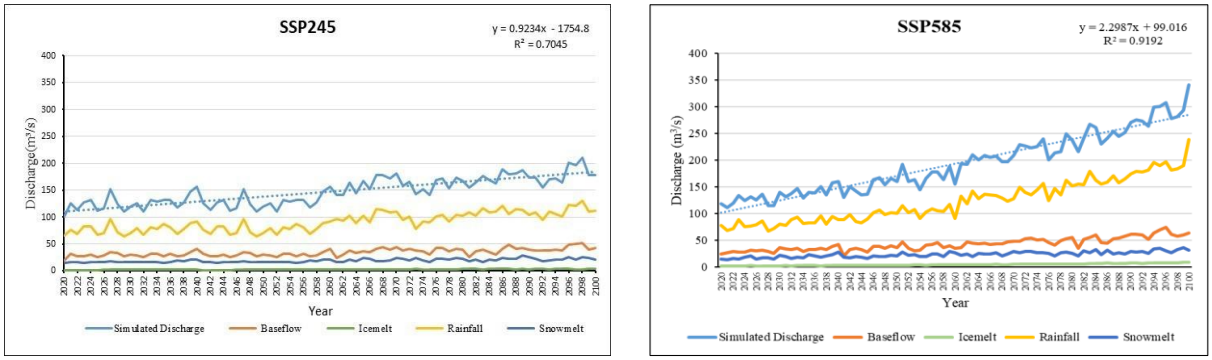

Figure. 6. Contribution of each component on total river discharge for 2020–2024 in projected future climate in BGRB.

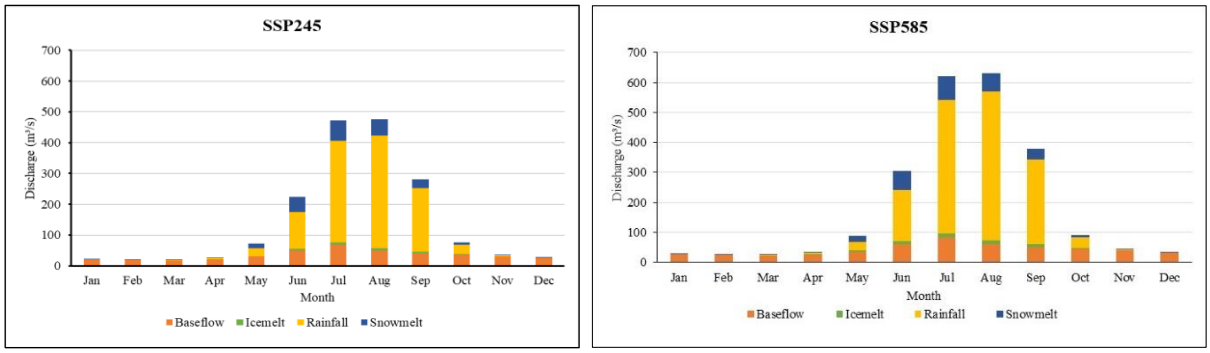

Figure. 7. Monthly contribution of Baseflow, Rainfall, Snow Melt, and Ice Melt to total river discharge in future projected scenarios for SSP2-4.5 and SSP5-8.5.

Conversely, in SSP5-8.5, although baseflow remains the highest contributor at 22.026 %, the percentage is slightly lower compared to SSP2-4.5. Rainfall remains a dominant factor at 63.81 %, indicating continued reliance on precipitation for water flow. However, there's a slight increase in the contribution of snow melt at 12.035 %, suggesting potential changes in snow dynamics due to climate scenarios associated with SSP5-8.5. Ice melt contributes 1.76 % in SSP2-4.5 and 2.12 % in SSP5-8.5, indicating its relatively minor role in the overall water flow.

These interpretations underscore the importance of considering different factors and scenarios when assessing water resource dynamics, especially in the context of changing climate conditions.

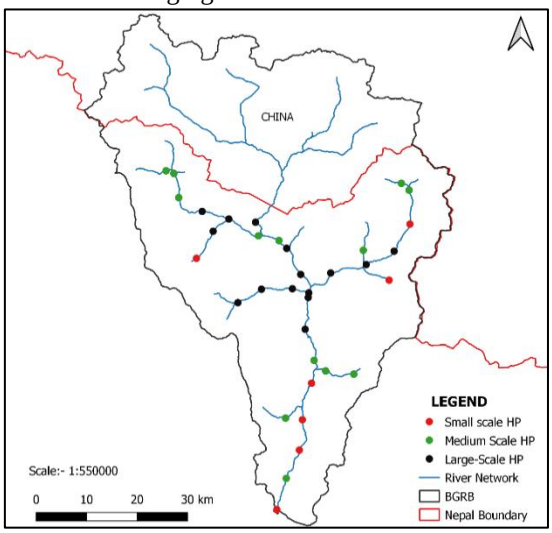

Figure 8. Hydropower sites classification based on production capacity, the points indicate the hydropower project's location, and the color ramp indicates its power potential.

5.4 Hydropower Potential Sites and Estimation

This study has identified 35 potential sites with an estimated total hydropower production capacity of around 6,308 MW. The spatial distribution of the identified 35 potential hydropower sites is shown in Figure 8. Jha, (2011) estimated a 3,286 MW capacity in BGRB using the hydropower model. Similarly, Bajracharya, (2015) estimated total potential of 6,743 MW using the mean annual flow and 30% of the dependable flow. The Bheri River basin, with a catchment area of 13,688 km², has an estimated hydropower potential of 4,142 MW, while the Marsyangdi River Basin offers 2,823 MW from 4,768 km² (Kayastha et al., 2024b). In contrast, our study estimates that the Budhigandaki River basin (BGRB), despite its smaller area of 3,881.16 km², possesses a higher potential of 6,308 MW. This can be attributed to the higher contribution of snowmelt in BGRB, accounting for 17.46 % of the total discharge, compared to only 7.8 % in Marsyangdi River basin. The greater snowmelt input, combined with the basin's steep topography and concentrated runoff, enhances its hydropower efficiency and overall energy generation capacity. Yusop et al., (2017) classified the capacity of hydropower into three classes, small hydropower (1-15) MW, medium hydropower (15-100) MW, and large hydropower (>100 MW). Among the 35 potential sites, this study identified eight small-scale hydropower sites, thirteen medium-scale, and fourteen large-scale sites. This study has found that 40 % of hydropower falls under large-scale hydropower whereas 37.1 % of hydropower falls under medium-scale.

6. Conclusion

GDM was successfully setup to estimate discharge from the Budhigandaki River basins. The model offers insights into the dynamics of the basin's hydrological system by providing data on baseflow (22.3 %), precipitation (40.57 %), snow melt (17.46 %), and ice melt (6.7 %). The NSE in river basins for the calibration and validation periods is between 0.84 to 0.86. In this study, a GIS-based spatial tool was selected for estimating hydro-power potential. During the hydropower potential evaluation, we found 35 potential sites. The estimated total hydro potential of BGRB is 6,308 MW at 40 % flow exceedance. Furthermore, the findings showed that small hydropower potential sites made up 22.9 % of all sites in the basin, with medium and high hydropower potential sites following closely behind with 37.1 % and 40 % of all sites each. The approach and findings might constitute the foundation for the development of a hydroelectric information system with geographical references, which could be used as a tool for energy-related decision-making.

The analysis of simulated discharge trends and the percentage contribution of various factors provide valuable insights into the future hydrological dynamics of the BGRB. The projected flow changes in the BGRB

under SSP2-4.5 and SSP5-8.5 from 2020 to 2100. SSP2-4.5 forecasts a modest 8.8 % increase to 148 m^3/s, attributed to moderate climate and human activity changes. In contrast, SSP5-8.5 anticipates a substantial 42.6 % rise to 194 m^3/s, indicating climate impacts and higher emissions. This scenario suggests heightened flood risks, altered water availability, and ecosystem impacts. SSP2-4.5 shows comparatively milder changes, indicating a less environmental impact. The research's findings offer insightful information. This study's calculated theoretical hydro potential has yielded the new potential value for Nepal's major rivers. The government and other interested parties will be able to create plans and strategies to grow hydropower in the nation with the use of this essential information. Additionally, during the desk research, the power developers might use this information to choose a certain river with a lot of potential.

Acknowledgment
Authors would like to thank Department of Hydrology and Meteorology, GoN, for providing hydro-meteorological data and the Himalayan Cryosphere, Climate and Disaster Risk Center, Department of Environmental Science and Engineering, for financial support and guidance.

Reference

Aryal, A., Magome, J., Pudashine, J. R., & Ishidaira, H. (2018). Identifying The Potential Location Of Hydropower Sites And Estimating The Total Energy In Bagmati River Basin. *Journal of Japan Society of Civil Engineers, Ser. G (Environmental Research)*, *74*(5), I_315-I_321. https://doi.org/10.2208/JSCEJER.74.I_315

Bajracharya, I. (2015a). *Assessment of run-of-river hydropower potential and power supply planning in Nepal using hydro resources*. https://doi.org/10.34726/HSS.2015.27916

Bajracharya, I. (2015b). Assessment of run-of-river hydropower potential and power supply planning in Nepal using hydro resources. *Institut Für Energietechnik Und Thermodynamike*, *April*, 7–12.

Barry, R. G. (2012). Recent advances in mountain climate research. *Theoretical and Applied Climatology*, *110*(4), 549–553. https://doi.org/10.1007/s00704-012-0695-x

Bhattarai, R., Mishra, B. K., Bhattarai, D., Khatiwada, D., Kumar, P., & Meraj, G. (2024). Assessing Hydropower Potential in Nepal's Sunkoshi River Basin: An Integrated GIS and SWAT Hydrological Modeling Approach. *Scientifica*, *2024*. https://doi.org/10.1155/2024/1007081

Bocchiola, D., Diolaiuti, G., Soncini, A., Mihalcea, C., D'Agata, C., Mayer, C., Lambrecht, A., Rosso, R., & Smiraglia, C. (2011). Prediction of future hydrological regimes in poorly gauged high altitude basins: The case study of the upper Indus, Pakistan. *Hydrology and Earth System Sciences*, *15*(7), 2059–2075. https://doi.org/10.5194/hess-15-2059-2011

Braithwaite, R. J., & Olesen, O. B. (1989). *Calculation of Glacier Ablation from Air Temperature, West Gre*. 219–233.

Calheiros, T., Beça, P., Capela Lourenço, T., Eggler, L., Mediavilla, M., Ferreras-Alonso, N., Ramos-Diez, I., Samsó, R., Distefano, T., & Pastor, A. (2024). Assessing Hydropower Potential under Shared Socioeconomic Pathways Scenarios Using Integrated Assessment Modelling. *Sustainability (Switzerland)*, *16*(4). https://doi.org/10.3390/su16041548

Shrestha, H. M. (1996). *H. M. Shrestha, "Cadastre of Potential Water Power Resources of Less Studied High Mountainous Regions, with Speical Reference to Nepal," Moscow Power Institute, USSR, Moscow, 1966. - References - Scientific Research Publishing*. https://www.scirp.org/reference/referencespapers?referenceid=883900

Halkos, G., & Gkampoura, E. C. (2023). Assessing Fossil Fuels and Renewables' Impact on Energy Poverty Conditions in Europe. *Energies*, *16*(1). https://doi.org/10.3390/en16010560

Immerzeel, W. W., Wanders, N., Lutz, A. F., Shea, J. M., & Bierkens, M. F. P. (2015). Reconciling high-altitude precipitation in the upper Indus basin with glacier mass balances and runoff. *Hydrology and Earth System Sciences*, *19*(11), 4673–4687. https://doi.org/10.5194/hess-19-4673-2015

Jha, R. (2010). Total Run-of-River type Hydropower Potential of Nepal. *Hydro Nepal: Journal of Water, Energy and Environment*, *7*(7), 8–13. https://doi.org/10.3126/HN.V7I0.4226

Jha, R. (2011). Total Run-of-River type Hydropower Potential of Nepal. *Hydro Nepal: Journal of Water, Energy and Environment*, *7*(January 2011), 8–13. https://doi.org/10.3126/hn.v7i0.4226

Joshi, T. P., & Mishra, B. K. (2024). Assessment of Run-of-River Hydropower Potential Using SWAT Modeling and GIS in the Marsyangdi River Basin, Nepal. *Journal of Hydrology and Meteorology*, *12*(1), 11–22. https://doi.org/10.3126/JHM.V12I1.72651

Kayastha, R. B., Ageta, Y., & Fujita, K. (2006). Use of Positive Degree-Day Methods for Calculating Snow and Ice Melting and Discharge in Glacierized Basins in the Langtang Valley, Central Nepal. *Climate and Hydrology in Mountain Areas*, 5–14. https://doi.org/10.1002/0470858249.ch2

Kayastha, R. B., & Kayastha, R. (2019). Glacio-hydrological degree-day model (gdm) useful for the himalayan river basins. *Himalayan Weather and Climate and Their Impact on the Environment*, 379–398. https://doi.org/10.1007/978-3-030-29684-1_19

Kayastha, R. B., Steiner, N., Kayastha, R., Mishra, S. K., & McDonald, K. (2020). Comparative Study of Hydrology and Icemelt in Three Nepal River Basins Using the Glacio-Hydrological Degree-Day Model (GDM) and Observations From the Advanced Scatterometer (ASCAT). *Frontiers in*

Earth Science, *7*(January), 1–13. https://doi.org/10.3389/feart.2019.00354

Kayastha, R., Kayastha, R. B., Shrestha, K. L., & Gurung, S. (2024a). Hydropower potential of the Marsyangdi River and Bheri River basins of Nepal and their sensitivity to climate variables. *Proceedings of IAHS*, *387*, 53–58. https://doi.org/10.5194/PIAHS-387-53-2024

Kayastha, R., Kayastha, R. B., Shrestha, K. L., & Gurung, S. (2024b). Hydropower potential of the Marsyangdi River and Bheri River basins of Nepal and their sensitivity to climate variables. 1966, 53–58.

Kouadio, C. A., Kouassi, K. L., Diedhiou, A., Obahoundje, S., Amoussou, E., Kamagate, B., Paturel, J. E., Coulibaly, T. J. H., Coulibaly, H. S. J. P., Didi, R. S., & Savane, I. (2022). Assessing the Hydropower Potential Using Hydrological Models and Geospatial Tools in the White Bandama Watershed (Côte d'Ivoire, West Africa). *Frontiers in Water*, *4*(March), 1–14. https://doi.org/10.3389/frwa.2022.844934

Luo, Y., Arnold, J., Allen, P., & Chen, X. (2012). Baseflow simulation using SWAT model in an inland river basin in Tianshan Mountains, Northwest China. *Hydrology and Earth System Sciences*, *16*(4), 1259–1267. https://doi.org/10.5194/hess-16-1259-2012

Marahatta, S. (2022). *Impacts of Climate Change on River Hydrology and Energy Economics in Budhigandaki River Basin*. *May*.

Marahatta, S., Aryal, D., Devkota, L. P., Bhattarai, U., & Shrestha, D. (2021). Application of swat in hydrological simulation of complex mountainous river basin (Part ii: Climate change impact assessment). *Water (Switzerland)*, *13*(11). https://doi.org/10.3390/w13111548

Marahatta, S., Devkota, L. P., & Aryal, D. (2021). Application of swat in hydrological simulation of complex mountainous river basin (Part i: Model development). *Water (Switzerland)*, *13*(11). https://doi.org/10.3390/w13111546

Mosier, T. M., Sharp, K. V., & Hill, D. F. (2016). The Hydropower Potential Assessment Tool (HPAT): Evaluation of run-of-river resource potential for any global land area and application to Falls Creek, Oregon, USA. *Renewable Energy*, *97*, 492–503. https://doi.org/10.1016/j.renene.2016.06.002

Nash, J. E., & Sutcliffe, J. V. (1970). River Flow Forecasting Through Conceptual Models - Part I - A Discussion of Principles. *Journal of Hydrology*, *10*(1970), 282–290.

Neitsch, S. L., Arnold, J. G., Kiniry, J. R., & Williams, J. R. (2011). Soil & Water Assessment Tool Theoretical Documentation Version 2009. *Texas Water Resources Institute*, 1–647. https://doi.org/10.1016/j.scitotenv.2015.11.063

Pandey, A., Lalrempuia, D., & Jain, S. K. (2015). Evaluation du potentiel hydroélectrique utilisant la technologie spatiale et le modèle SWAT pour la rivière Mat, dans le sud Mizoram, Inde. *Hydrological Sciences Journal*, *60*(10), 1651–1665. https://doi.org/10.1080/02626667.2014.943669

Pokharel, N., Basnet, K., Sherchan, B., & Thapaliya, D. (2020). *Assessment of Hydropower Potential using SWAT modeling and Spatial Technology in the Seti Gandaki River, Kaski, Nepal*. *8*(7), 87–102.

Pradhan, P. M. S. (2009). Hydropower Development. *The Nepal-India Water Relationship: Challenges*, 125–151. https://doi.org/10.1007/978-1-4020-8403-4_5

Prajapati, R. N. (2015). Delineation of Run of River Hydropower Potential of Karnali Basin-Nepal Using GIS and HEC-HMS. *European Journal of Advances in Engineering and Technology*, *2*(1), 50–54.

Kayastha, R. B. (2019). Glacio-hydrological degree-day model (gdm) useful for the himalayan river basins. *Himalayan Weather and Climate and Their Impact on the Environment*, 379–398. https://doi.org/10.1007/978-3-030-29684-1_19

Sharma, T. P., Pangali, Zhang, J., Khanal, N. R., Prodhan, F. A., Paudel, B., Shi, L., & Nepal, N. (2020). Assimilation of Snowmelt Runo ff Model (SRM) Using Satellite Remote Sensing Data in Budhi. *Remote Sens*, *12*(1951), 1–21.

Spanoudaki, K., Dimitriadis, P., Varouchakis, E. A., & Corzo Perez, G. A. (2022). Estimation of Hydropower Potential Using Bayesian and Stochastic Approaches for Streamflow Simulation and Accounting for the Intermediate Storage Retention. *Energies*, *15*(4). https://doi.org/10.3390/en15041413

Sperna Weiland, F. C., Van Beek, L. P. H., Kwadijk, J. C. J., & Bierkens, M. F. P. (2010). The ability of a GCM-forced hydrological model to reproduce global discharge variability. *Hydrology and Earth System Sciences*, *14*(8), 1595–1621. https://doi.org/10.5194/hess-14-1595-2010

WECS. (2011). Government of Nepal Water and Energy Commission Secretariat Water resources of Nepal in the context of climate change.

WECS. (2019). Assessment of Hydropower Potential of Nepal Final Report.

Yusop, A., Yahaya, I., Kadis, G., Ishak, M., Abdullah, M. S., Razak, M. F., Sidek, A., & Abdul Rahman, I. (2017). Hybrid Micro-Hydro Power Generation Development in Endau Rompin National Park Johor, Malaysia. *MATEC Web of Conferences*, *135*. https://doi.org/10.1051/matecconf/201713500007

Zhang, Y., Hirabayashi, Y., Liu, Q., & Liu, S. (2015). Glacier runoff and its impact in a highly glacierized catchment in the southeastern Tibetan Plateau: Past and future trends. *Journal of Glaciology*, *61*(228), 713–730. https://doi.org/10.3189/2015JoG14J188

Zhang, Y., Ma, H., & Zhao, S. (2021). Assessment of hydropower sustainability: Review and modeling. *Journal of Cleaner Production*, *321*(August), 128898. https://doi.org/10.1016/j.jclepro.2021.128898